

Received August 11, 2019, accepted August 23, 2019, date of publication August 27, 2019, date of current version September 11, 2019.

Digital Object Identifier 10.1109/ACCESS.2019.2937849

4-Bit Optimized Coding Metasurface for Wideband RCS Reduction

YASIR SAIFULLAH¹, (Student Member, IEEE), ABU BAKAR WAQAS,
GUO-MIN YANG¹, (Senior Member, IEEE), FUHENG ZHANG¹,
AND FENG XU¹, (Senior Member, IEEE)

Key Laboratory for Information Science of Electromagnetic Waves (MoE), Fudan University, Shanghai 200433, China

Corresponding author: Guo-Min Yang (guominyang@fudan.edu.cn)

This work was supported in part by the National Key Research and Development Program of China under Grant 2017YFA0100203, and in part by the NSFC under Grant 61571130, Grant 61822107, and Grant U1637213.

ABSTRACT In this paper, a 4-bit reflective coding metasurface with the polarization-insensitive unit cell is designed for wideband radar cross section (RCS) reduction. The metasurface unit has rotational symmetry; therefore, it produces the same electromagnetic scattering response for both x- and y-polarizations. To attain 4-bit phase response, the dimensions of the unit cell are optimized so that a phase difference of 22.5° is realized between respective digital elements and the magnitude of reflection is more than 0.95 from 15 GHz to 40 GHz. Therefore, 16 digital elements have phases of θ , $\theta + 22.5^\circ$, $\theta + 45^\circ$, $\theta + 67.5^\circ$, $\theta + 90^\circ$, $\theta + 112.5^\circ$, $\theta + 135^\circ$, $\theta + 157.5^\circ$, $\theta + 180^\circ$, $\theta + 202.5^\circ$, $\theta + 225^\circ$, $\theta + 247.5^\circ$, $\theta + 270^\circ$, $\theta + 292.5^\circ$, $\theta + 315^\circ$, and $\theta + 337.5^\circ$. Discrete water cycle algorithm (DWCA) is applied to the array factor to get the optimal coding sequence matrix for better RCS reduction. The coding metasurface can achieve more than 10 dB RCS reduction from 15 GHz to 40 GHz as compared with the same size of a copper sheet. The simulation and experiment results validate the ability of proposed coding metasurface for robust control of EM-wave and wideband RCS reduction.

INDEX TERMS 4-bit, coding, discrete water cycle algorithm, metasurface, reflective, radar cross section (RCS).

I. INTRODUCTION

With the rapid advancements of defense electronics, the demand for stealth technology is increased drastically in recent years. Radar cross section (RCS) of a flying object is an essential factor that evaluates its visibility to radar. Therefore, the stealth aircraft should have a low radar signature to decrease the detection probability. The traditional stealth technology is based on the coating of the object with radar absorbing material (RAMs) [1] and changing its shape [2]–[4]. The radar absorbing material increases the weight and thickness of the object, whereas the shape stealth technique makes the design more intricate and affects the aerodynamic layout.

The metasurface is a kind of subwavelength structure, which manipulate the EM waves in a controlled manner to obtain electromagnetic characteristics that are unavailable in natural materials. The metasurface is more advantageous

as compared to 3D metamaterial for diverse applications because of easy fabrication, low complexity, and less thickness. Although periodicity is not an essential condition for metasurface, yet many designs are based on repeated unit cells to arbitrarily control wave propagations, scattering, and polarization [5]. For the last two decades, metamaterials have been used for many applications, including electromagnetic cloak [6]–[8], negative refraction [9], subwavelength focusing [10], beam manipulation [11] and perfect absorber [12].

Recently, digital metamaterials are introduced by C. Giovampaola *et al.* that brings a new concept of controlling the EM response of metasurface unit cell as digital bits [13] which is different from the effective-medium theory of conventional metamaterials. T. J. Cui *et al.* enhanced this concept of digital metamaterials by introducing the coding and programmable metasurface [14]. The coding bits consist of 0° and 180° phase response, which are considered as “0” and “1” element of coding metasurface. The unit cells are arranged to construct an array, and by changing the coding sequence of the metasurface, diverse EM functionalities can

The associate editor coordinating the review of this article and approving it for publication was Ildiko Peter.

be achieved. It is worth mentioning that digital metasurface combines the digital codes with physical particles and therefore extend the metasurface applications to digital signal processing and information theory [15]. Coding metasurface has attracted significant attention in recent years, and many designs of coding metasurface have been proposed for broadband RCS reduction. The simplest case is the 1-bit coding metasurface [16], the ‘0’ element of the digital metasurface is designed with 0° phase response and ‘1’ element with 180° phase response. The opposite phase cancellation has been adopted to reduce RCS [17], wherein the phase difference of $180^\circ \pm 37^\circ$ is maintained for a specific frequency range. In [18], a 2-bit coding metasurface with four digital states is presented for RCS reduction at THz frequencies. In [19], a 3-bit polarization conversion metasurface was presented for wideband RCS reduction.

Several designs of the artificial magnetic conductor (AMC) with unit cells having opposite phase responses are designed in chessboard arrangement to cancel the specular reflection, and as a result, the radar cross section (RCS) has been reduced [20]–[22]. The AMC with chessboard arrangement has a drawback of narrow bandwidth. To achieve the wideband RCS reduction, Li *et al.* in [23] used a two-dimensional phase gradient metasurface. A spiral coded metasurface was introduced by F. Yuan *et al.* for broadband RCS reduction [24]. S. Sui *et al.* in [25] have presented absorptive metasurface to redirect the EM-wave in a different direction. A 3-bit reflective coding metasurface was designed using a random combination of unit cells [26]. These designs are based on diffusion metasurface by random arrangements of unit cells; hence, the array pattern is suboptimal. For better RCS reduction, the optimized metasurface arrangements are introduced in [27]–[30] by using 1-bit coding metasurface. Genetic algorithm (GA) or binary particle swarm optimization (BPSO) is implemented for optimized metasurface array design. Binary optimization algorithms are useful for 1-bit coding metasurface because there are only two possible states, “0” or “1”. In this paper, a 4-bit coding metasurface is introduced, which has 16 digital states. Binary optimization techniques are not applicable for 4-bit metasurface; therefore, a discrete water cycle algorithm DWCA is applied in this paper which can optimize the 16 digital states.

In this article, a 4-bit reflective coding metasurface with the polarization-insensitive unit cell is presented and characterized for wideband radar cross section (RCS) reduction. To achieve a 4-bit phase response, the size of the unit cell is optimized so that a phase difference of 22.5° is realized between respective digital elements. Discrete water cycle algorithm is applied to array factor to get the optimal coding sequence matrix for a better RCS reduction. The coding metasurface can achieve more than 10 dB RCS reduction from 15 GHz to 40 GHz as compared with the same size of a copper sheet. The simulation and experiment results validate the ability of the proposed coding metasurface for robust control of EM-wave and wideband RCS reduction.

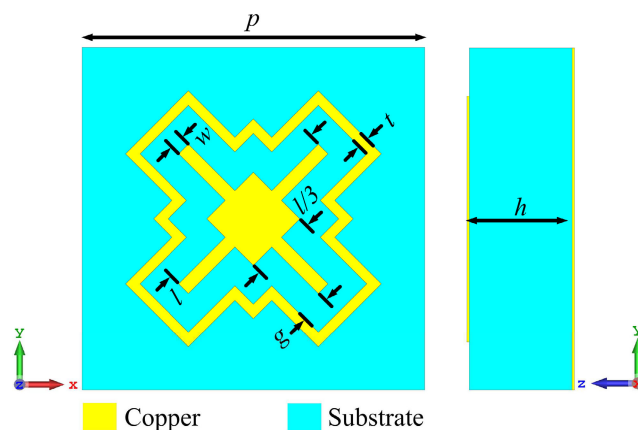


FIGURE 1. Schematic of the proposed unit cell. Here, $p = 5$ mm, $w = 0.2$ mm, $t = 0.15$ mm, $g = 0.4$ mm.

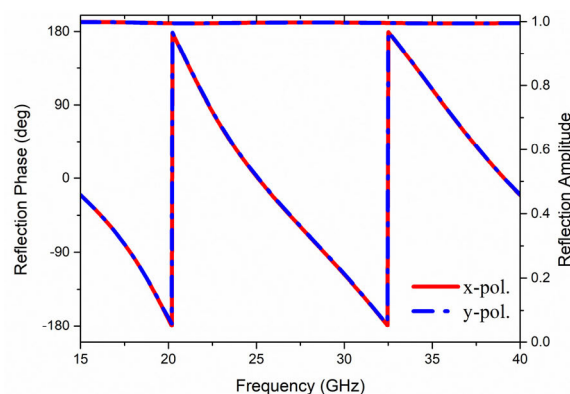


FIGURE 2. Simulation results of reflection phase and magnitude of the proposed unit cell.

II. UNIT CELL DESIGN AND ANALYSIS

The schematic model of the proposed unit cell is presented in Fig.1. The unit cell is a sandwich structure with the top, and the bottom layer is copper while the middle layer is a dielectric substrate. The dielectric substrate F4B ($\epsilon_r = 2.65$ and $\tan \delta = 0.001$) has a thickness of 1.5 mm and periodicity of the unit cell is 5 mm. The thickness of top metal patches and ground is 0.035 mm.

Because of the rotational symmetry of the unit cell, it produces the same electromagnetic scattering for both x- and y-polarizations, which is vital for the polarization-insensitive response. The periodic boundary and Floquet port are applied for the unit cell simulations in CST Microwave Studio and frequency domain solver is used. The phase and magnitude response of the proposed unit cell from 15 GHz to 40 GHz is presented in Fig. 2. The metasurface unit cell with multiple resonance design is necessary for the wideband operation. The phase and magnitude responses of 4-bit coding metasurface are illustrated in Fig. 3 and Fig. 4, respectively. The sixteen curves show the phase of each unit cell of the metasurface. Each unit cell of the coding metasurface exhibits a

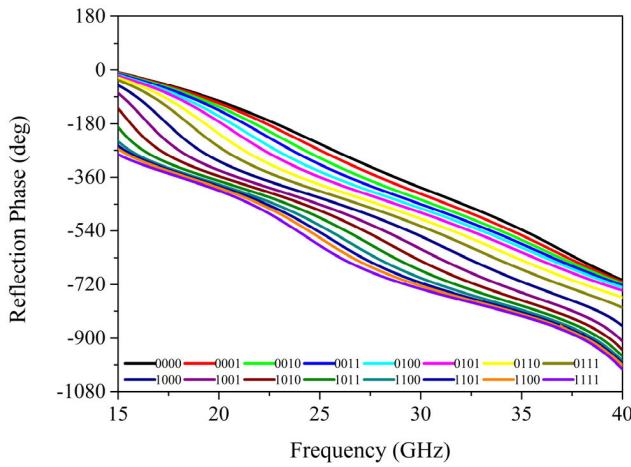


FIGURE 3. The phase response of unit cells vs. frequency with a change in unit cell length l .

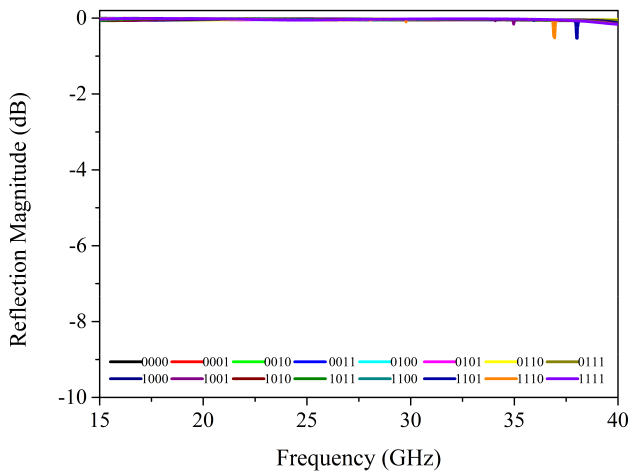


FIGURE 4. The magnitude response of unit cells vs. frequency with a change in unit cell length l .

linear response for broadband (15 GHz-40 GHz), and phase difference of $22.5^\circ + \theta$ is achieved between respect states of metasurface unit cell. The proposed unit cell is designed as a dual resonance structure to accomplish a wide-band operation.

The unit cell is optimized such that the resonance points are out of working band to get a better reflection magnitude in the operating frequency band (15 GHz-40 GHz). The first resonance point is before 15 GHz and the second resonance point is after 40 GHz; therefore, the reflection amplitude value is more than 0.95 for all 16 states of the metasurface unit cell as shown in Fig. 4. To achieve the 4-bit coding metasurface, the reflection phases at $0^\circ, 22.5^\circ, 45^\circ, 67.5^\circ, 90^\circ, 112.5^\circ, 135^\circ, 157.5^\circ, 180^\circ, 202.5^\circ, 225^\circ, 247.5^\circ, 270^\circ, 292.5^\circ, 315^\circ$ and 337.5° as $l = 1.50$ mm, 1.60 mm, 1.70 mm, 1.80 mm, 1.94 mm, 2.08 mm, 2.26 mm, 2.48 mm, 2.66 mm, 2.88 mm, 2.96 mm, 3.08 mm, 3.18 mm, 3.32 mm, 3.44 mm, and 3.56 mm, respectively.

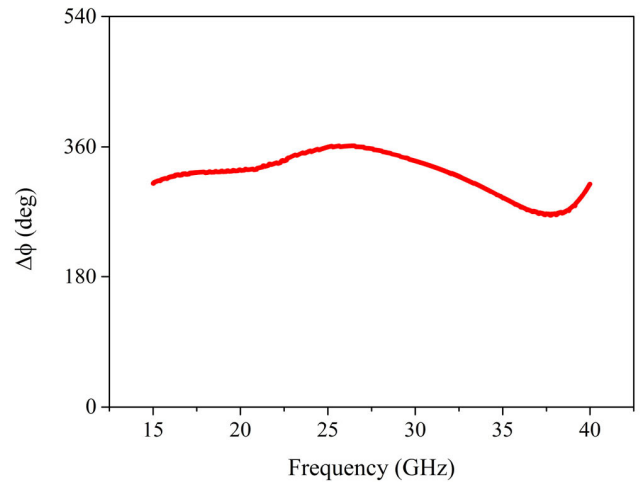


FIGURE 5. The accessible phase range for the proposed unit cell from 15 GHz to 40 GHz.

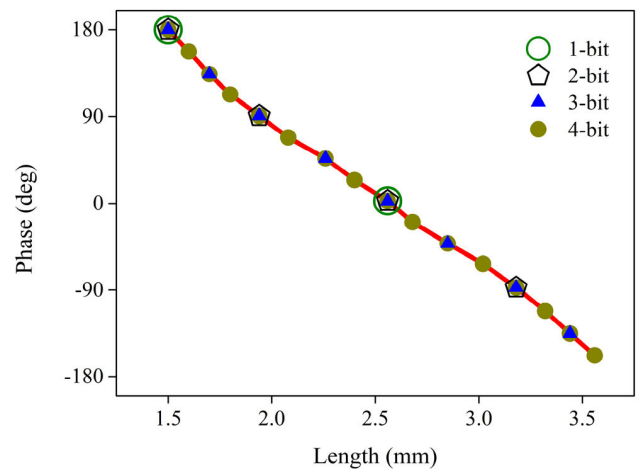






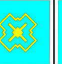
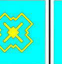
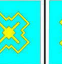
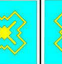


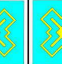
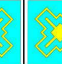
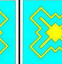
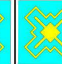
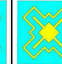

FIGURE 6. The relation of the phase with unit cell length l .

The proposed design can be used for 1-bit, 2-bit, 3-bit, and 4-bit coding metasurface by proper selection of unit cell's length L as illustrated in Table 1. To attain better control of the scattering patterns, the phase range of the proposed unit cell is calculated by changing the width at different frequencies as shown in Fig. 5. Because of the multi-resonance structure, the phase coverage of more than 280° is observed from 15 GHz to 40 GHz. To design the unit cell of coding metasurface, the reflection phase variation with respect to the length of the unit cell is shown in Fig. 6. It is evident from the figure that phase has a linear relation to the length l of the unit cell, which is the most critical design parameter using the same geometry.

III. OPTIMIZED ARRAY DESIGN

Once the metasurface unit cell is designed and optimized, we are going to arrange these unit cells to construct an array. The simplest array is formed by 1-bit coding metasurface with two digital elements that are placed in an alternative

TABLE 1. The designed 1-, 2-, 3-, and 4- bit coding metasurface using different size of unit cell.

Phase and shape	0°	22.5°	45°	67.5°	90°	112.5°	135°	157.5°	180°	202.5°	225°	247.5°	270°	292.5°	315°	337.5°
Multi-bit																
1-bit	0								1							
2-bit	00				01				10				11			
3-bit	000		001		010		011		100		101		110		111	
4-bit	0000	0001	0010	0011	0100	0101	0110	0111	1000	1001	1010	1011	1100	1101	1110	1111

arrangement to get two beams. The chessboard structure is based on the principle of destructive interference, the incident wave is divided into four beams, and the backscattering in specular direction is minimized. The chessboard structure has a drawback of narrow bandwidth, so it is not suitable for broadband RCS reduction application. The diffusion metasurface was introduced that randomly disperse the scattering waves and has better working bandwidth, but the problem with this metasurface is the lack of optimization.

By using the optimization algorithm for unit cell arrangement, better RCS reduction could be achieved. For $M \times N$ array of metasurface unit cells, the far-field is illustrated by the following equation

$$E_{total} = EP \times AF$$

where E_{total} is the scattering far-field, AF is the array factor, and EP is the pattern of the individual unit cell. For a rectangular array of $M \times N$ uniformly spaced elements, the array factor is expressed as follow,

$$AF = \sum_{m=1}^M \sum_{n=1}^N \exp \{ jkd [(m - 0.5) \sin \theta \cos \varphi + (n - 0.5) \sin \theta \sin \varphi] + j\theta(m, n) \}$$

where d is the periodicity of the unit cell, θ is elevation angle, φ is azimuth angle, $j\theta(m, n)$ is the phase of individual unit cell which could be one of the 16 value of phase $0^\circ, 22.5^\circ, 45^\circ, 67.5^\circ, 90^\circ, 112.5^\circ, 135^\circ, 157.5^\circ, 180^\circ, 202.5^\circ, 225^\circ, 247.5^\circ, 270^\circ, 292.5^\circ, 315^\circ$ and 337.5° in case of 4-bit metasurface.

The metasurface array can be considered as $M \times N$ matrix, where M and N is the number of unit cells along x - and y -axis, respectively. In order to get the low RCS, the discrete water cycle algorithm [31] is applied to array factor to get the optimal coding sequence matrix, as shown in Fig. 7. The fitness function for this optimization problem is given by

$$fitness = \min(AF_{max})$$

The water cycle algorithm is applied to minimize the array factor (AF) at 24 GHz to obtain the optimal solution for

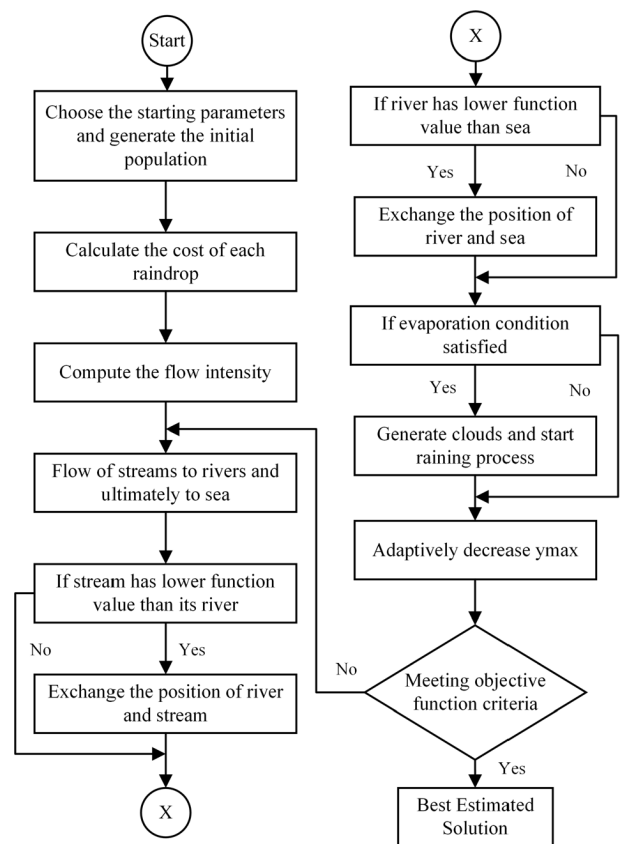


FIGURE 7. Flow chart of water cycle algorithm.

RCS reduction. The convergence characteristics of discrete water cycle algorithm (DWCA) is shown in Fig. 8 (a), the algorithm is applied for 200 iterations, and the optimized value of array factor is achieved. The simulation results of 2D and 3D far-field patterns of the proposed metasurface are presented in Fig. 8(b) and Fig. 8(c), respectively. The algorithm is applied in MATLAB to attain the best solution for the array matrix, as shown in Fig. 9, and then this optimum coding matrix is used to form an array of unit cells for better RCS reduction. The optimized array design, according to

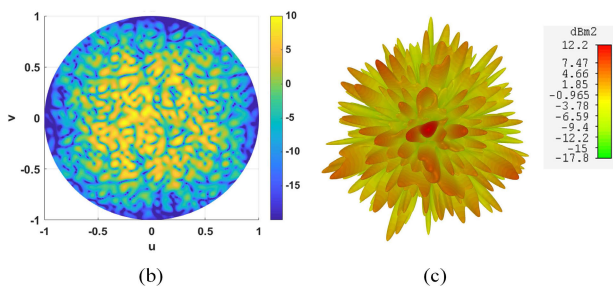
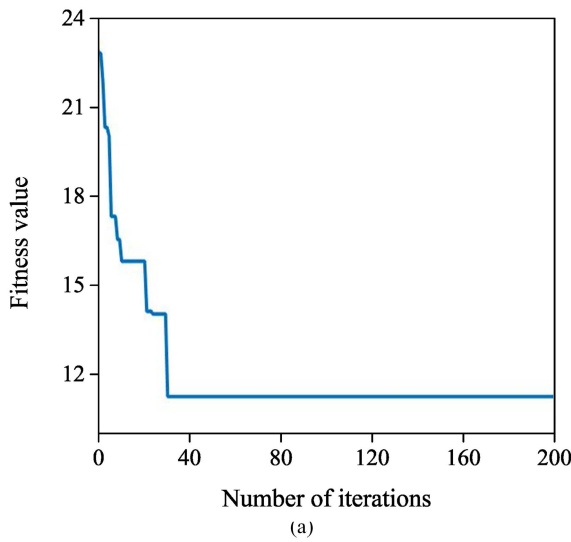


FIGURE 8. (a) Convergence characteristics of Discrete water cycle algorithm. (b) 2D scattering pattern of the metasurface. (c) 3D scattering pattern of the optimized metasurface.

the optimized coding matrix, is presented in Fig. 10. The backscattered characteristic of PEC and optimized coding metasurface is investigated by comparing the E-field distribution. It is evident from Fig. 11 that optimized coding metasurface has more diffused scattering than PEC.

To validate the RCS performance of metasurface, the far-field pattern is computed at 15 GHz, 24 GHz, and 40 GHz. CST Microwave Studio is used for full-wave simulation of the array of coding metasurface, and results are presented in Fig. 13. The 4-bit optimized coding metasurface has RCS of 12.2 dBsm, 10.4 dBsm, and 16.8 dBsm at 15 GHz, 24 GHz, and 40 GHz, respectively. The 16-unit cells of metasurface present distinct phase response, which is useful for altering the uniform phase response of the array. The phase distribution of the adjacent unit cell is nonuniform; therefore, the specular reflection is not dominant in a backscattered wave. The optimized coding reflective metasurface distributed the backscattered wave in many directions and suppressed the amplitude of the main beam. The far-field pattern for coding metasurface shows diffusion scattering pattern as compared to PEC in which most of the energy is present in the single lobe. The RCS reduction of 13.3 dBsm, 18.8 dBsm, and 16.9 dBsm as compared to PEC is observed at 15 GHz, 24 GHz, and 40 GHz, respectively. Therefore, the RCS of the

9	3	6	14	1	10	3	2	1	7	6	0	13	1	9	15
5	4	12	15	11	9	15	11	0	2	8	11	1	13	8	7
14	11	12	5	15	4	14	3	8	8	11	10	5	14	2	13
6	15	15	9	11	9	7	1	13	15	2	2	5	2	9	1
12	13	3	13	7	12	3	8	10	7	8	4	11	3	10	15
2	7	11	0	2	8	10	7	5	0	10	7	14	14	4	5
9	14	6	3	11	10	11	6	11	15	13	4	14	11	5	11
8	2	15	6	14	9	12	4	13	9	3	13	2	15	4	5
13	12	1	15	5	14	7	2	8	0	11	3	6	14	9	9
3	14	4	9	4	10	9	15	6	6	8	7	5	3	6	2
5	8	12	15	10	11	12	9	6	11	8	10	14	3	4	3
3	13	5	11	7	14	0	13	6	12	13	10	1	6	15	10
9	10	0	9	3	0	14	9	10	12	6	15	11	15	8	5
12	6	2	15	10	10	6	13	2	5	12	9	15	3	11	14
3	6	13	4	14	14	3	6	9	0	13	3	4	0	3	1
11	10	5	7	1	11	2	11	15	1	3	12	15	6	15	0

FIGURE 9. Optimized unit cell distribution for array formation.

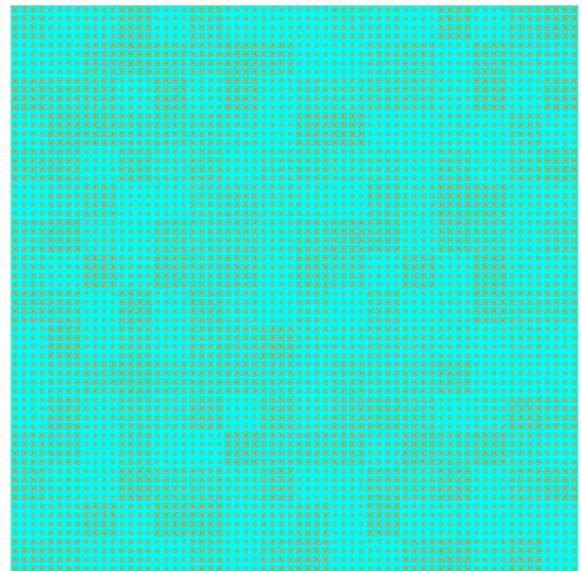


FIGURE 10. The layout of the 4-bit optimized coding metasurface array.

coding metasurface is much lower than the equal size PEC. It is worth mentioning that the scattering beams have close concentrations at higher frequencies because the periodicity of the array factor reduces with the increase of frequency. The scattering pattern of the metasurface is different at different frequency because of the varying phase layout response of metasurface with the change in frequency. To analyze the wideband RCS reduction performance of the coding metasurface, the comparison between PEC and optimized coding metasurface from 15 GHz to 40 GHz is presented in Fig. 14. As shown in the figure, the RCS reduction performance is similar for both x- and y-polarizations. The simulation results show that more than 10 dB RCS reduction is achieved, by using 4-bit coding metasurface, from 15 GHz to 40 GHz

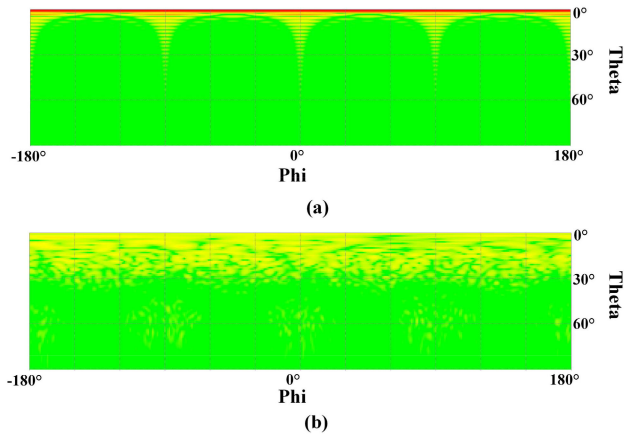


FIGURE 11. E-field distribution at 24 GHz of (a) PEC (b) 4-bit optimized coding metasurface.

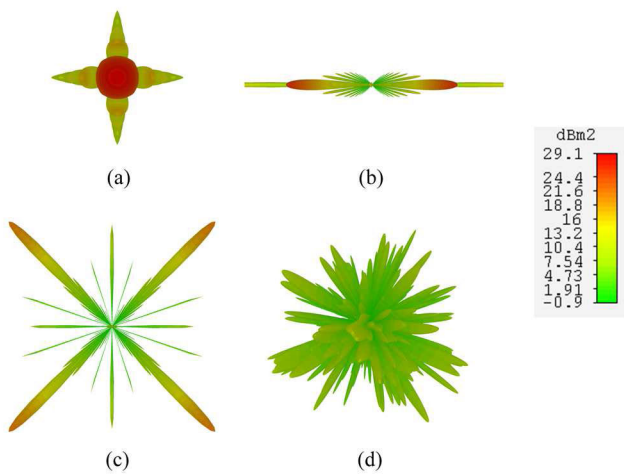


FIGURE 12. The scattering pattern of different arrangements. (a) All “0” elements. (b) The distribution of “0” and “1” in an alternative arrangement. (c) The distribution of “0” and “1” in chessboard arrangement. (d) The optimized coding metasurface.

except for 17 GHz to 18 GHz, where RCS reduction is more than 7.8 dB. The maximum RCS reduction of 18.8 dBsm is observed at the frequency of 24 GHz.

IV. FABRICATION AND MEASUREMENTS

To validate the performance, a sample of 4-bit coding metasurface is fabricated, as shown in Fig. 15. The sample was fabricated using printed circuit board technology. The metasurface array comprises of a top metallic patch, a substrate, and a metal ground. The substrate used here is F4B ($\epsilon_r = 2.65$ and $\tan \delta = 0.001$) with a thickness of 1.5 mm. The thickness of top metal patches and ground is 0.035 mm. The experiment is performed in an anechoic chamber as illustrated in Fig. 16. The distance between the sample and the horn antenna is taken to satisfy the far-field condition. Three sets of horn antennas were used to cover the band of 15-18 GHz, 18-26.5 GHz, and 26.5-40 GHz. The transmitting and

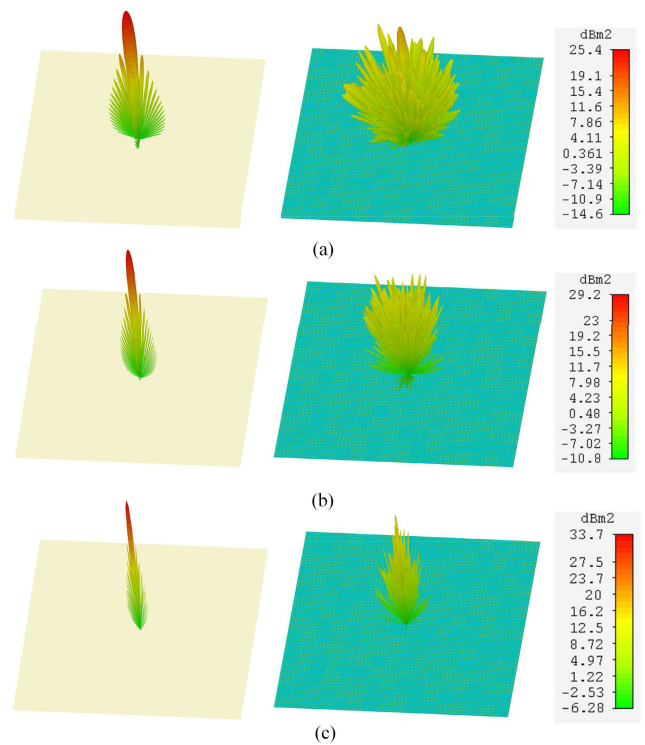


FIGURE 13. The scattering patterns of the metal (left column) and the 4-bit coding metasurface (right column) in 3D at (a) 15 GHz, (b) 24 GHz, and (c) 40 GHz.

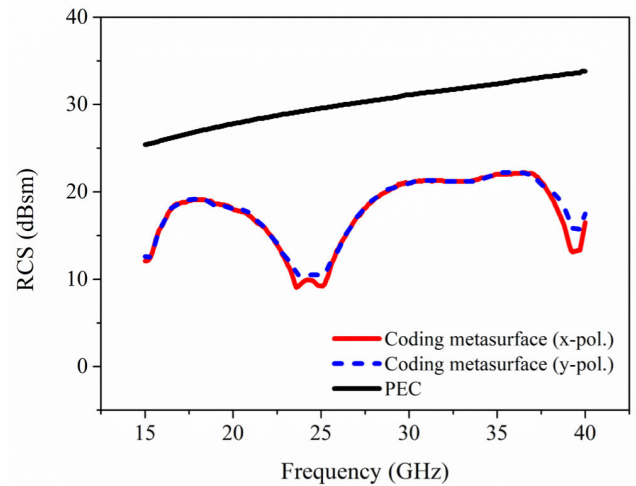


FIGURE 14. The RCS of PEC and coding metasurface for TE and TM polarizations.

receiving antennas are connected at two ports of vector network analyzer (Agilent N5227A).

The comparison of simulation and measured results of the backward-reflection as a function of frequency is depicted in Fig. 17. The RCS result of coding metasurface is compared with the same size as the copper sheet. The coding metasurface can achieve more than 10 dB RCS reduction from 15 GHz to 40 GHz except for 17 GHz

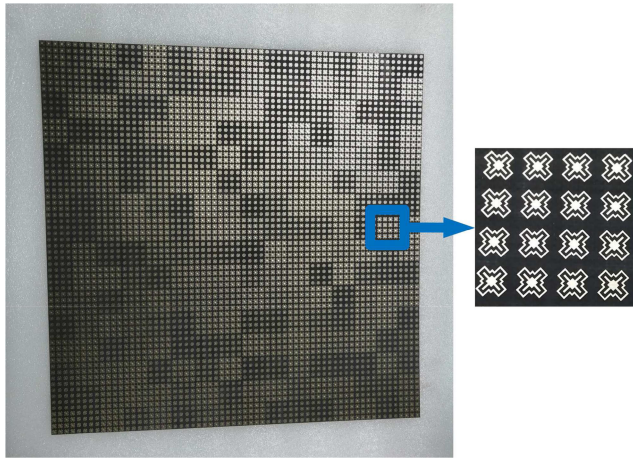


FIGURE 15. The fabricated sample of propose metasurface.

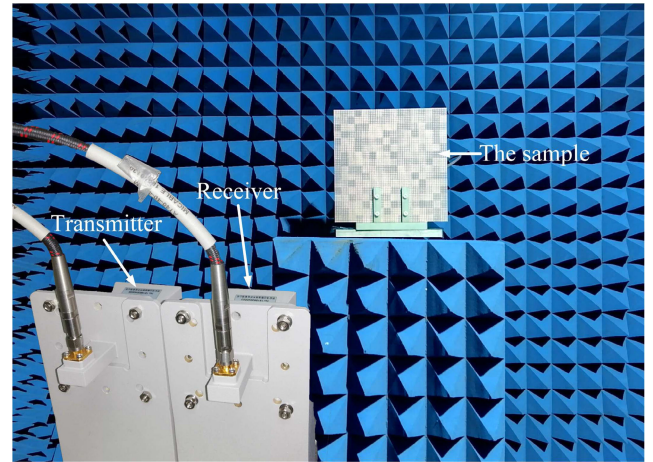


FIGURE 16. Experimental setup in an anechoic chamber.

TABLE 2. Comparison of our work with previous works.

Ref.	Thickness	Metasurface arrangement	σ_R (dB)	Freq. band (GHz)	FBW (%)	RBW
[19]	$0.13\lambda_0$	Random	10	8-18	77	2.25
[24]	$0.12\lambda_0$	Spiral coding	10	12.2-23.4	62	1.91
[28]	$0.12\lambda_0$	GA	10	12-24	66	2.00
[29]	$0.14\lambda_0$	GA	10	5.8-12.2	77	2.10
[30]	$0.21\lambda_0$	GA	10	4.8-16.4	109	3.40
[32]	$0.31\lambda_0$	Chessboard	10	10.5-18	52	1.71
[33]	$0.12\lambda_0$	Random	10	7.2-15.6	73	2.10
[34]	$0.15\lambda_0$	Random	10	9.9-19.8	66	2.00
[35]	$0.13\lambda_0$	Checkerboard	10	4.1-7.6	63	1.85
[36]	$0.23\lambda_0$	Checkerboard	10	7.5-13.2	55	1.76
[37]	$0.14\lambda_0$	Checkerboard	10	9.3-15.5	50	1.67
This work	$0.13\lambda_0$	DWCA	10	15-40	91	2.66

λ_0 is the free-space wavelength corresponding to the center frequency of the operation bandwidth.

σ_R : RCS reduction

FBW: The fractional bandwidth

$FBW = (f_H - f_L) / f_c, f_c = (f_H + f_L) / 2$

RBW: The ratio bandwidth ($RBW = f_H / f_L$)

to 18 GHz where RCS reduction is more than 7.8 dB. The small deviation between simulation and measured results is considered as fabrication error and measurement tolerance.

The comparison of this paper with previous research is presented in Table 2. The proposed design has an advantage in the bandwidth expansion of RCS reduction with a ratio bandwidth (RBW) of 2.6:1 and fractional bandwidth (FBW) of 91% and also has less thickness ($0.13\lambda_0$) which contributes to lower weight as well as less cost. Binary optimization techniques are not applicable for 4-bit metasurface, therefore a discrete optimization algorithm DWCA is applied in this paper to optimize the 16 digital states.

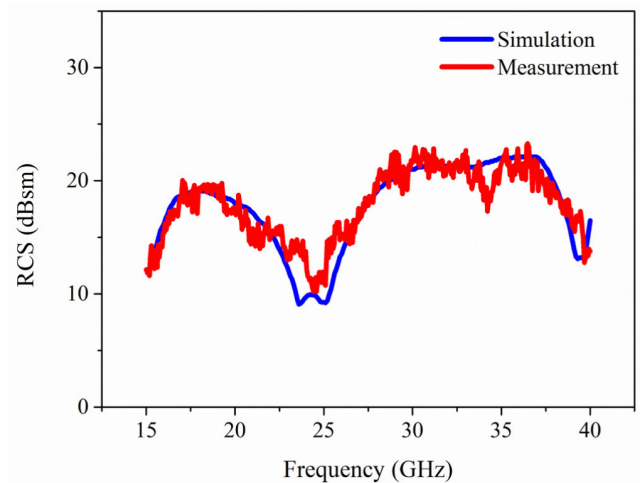


FIGURE 17. Comparison of simulation and measurement results.

V. CONCLUSION

A 4-bit reflective coding metasurface with the polarization-insensitive unit cell is presented for wideband radar cross section (RCS) reduction. To attain 4-bit phase response, the dimensions of the unit cell are optimized in such a way that a phase difference of 22.5° is realized between respective digital elements and magnitude of reflection is more than 0.95 from 15 GHz to 40 GHz. Discrete water cycle algorithm is applied to array factor to get the optimal coding sequence matrix for better RCS reduction. The proposed metasurface has achieved more than 10 dB RCS reduction from 15 GHz to 40 GHz. The simulation and measurement results validate the ability of 4-bit coding metasurface for robust control of EM-wave and wideband RCS reduction.

REFERENCES

- [1] X. Liu, T. Starr, A. F. Starr, and W. J. Padilla, "Infrared spatial and frequency selective metamaterial with near-unity absorbance," *Phys. Rev. Lett.*, vol. 104, no. 20, p. 207403, 2010.

- [2] W. F. Bahret, "The beginnings of stealth technology," *IEEE Trans. Aerosp. Electron. Syst.*, vol. 29, no. 4, pp. 1377–1385, Oct. 1993.
- [3] P. Y. Ufimtsev, "New insight into the classical Macdonald physical optics approximation," *IEEE Antennas Propag. Mag.*, vol. 50, no. 3, pp. 11–20, Jun. 2008.
- [4] E. F. Knott, *Radar Cross Section Measurements*, 1st ed. New York, NY, USA: Springer, 1993.
- [5] H. Yang, X. Cao, F. Yang, J. Gao, S. Xu, M. Li, X. Chen, Y. Zhao, Y. Zheng, and S. Li, "A programmable metasurface with dynamic polarization, scattering and focusing control," *Sci. Rep.*, vol. 6, Oct. 2016, Art. no. 35692.
- [6] D. Schurig, J. J. Mock, B. J. Justice, S. A. Cummer, J. B. Pendry, A. F. Starr, and D. R. Smith, "Metamaterial electromagnetic cloak at microwave frequencies," *Science*, vol. 314, no. 5801, pp. 977–980, Nov. 2006.
- [7] R. Liu, C. Ji, J. J. Mock, J. Y. Chin, T. J. Cui, and D. R. Smith, "Broadband ground-plane cloak," *Science*, vol. 323, no. 5912, pp. 366–369, Jan. 2009.
- [8] H. F. Ma and T. J. Cui, "Three-dimensional broadband ground-plane cloak made of metamaterials," *Nature Commun.*, vol. 1, p. 21, Jun. 2010.
- [9] D. R. Smith, J. B. Pendry, and M. C. K. Wiltshire, "Metamaterials and negative refractive index," *Science*, vol. 305, no. 5685, pp. 788–792, 2004.
- [10] J. Pendry, "Negative refraction makes a perfect lens," *Phys. Rev. Lett.*, vol. 85, no. 18, p. 3966, 2000.
- [11] M. I. Shalaev, J. Sun, A. Tsukernik, A. Pandey, K. Nikolskiy, and N. M. Litchinitser, "High-efficiency all-dielectric metasurfaces for ultra-compact beam manipulation in transmission mode," *Nano Lett.*, vol. 15, no. 9, pp. 6261–6266, 2015.
- [12] N. I. Landy, S. Sajuyigbe, J. J. Mock, D. R. Smith, and W. J. Padilla, "Perfect metamaterial absorber," *Phys. Rev. Lett.*, vol. 100, May 2008, Art. no. 207402.
- [13] C. D. Giovampaola and N. Engheta, "Digital metamaterials," *Nature Mater.*, vol. 13, no. 12, pp. 1115–1121, Sep. 2014.
- [14] T. J. Cui, M. Q. Qi, X. Wan, J. Zhao, and Q. Cheng, "Coding metamaterials, digital metamaterials and programmable metamaterials," *Light Sci. Appl.*, vol. 3, no. 10, p. e218, Oct. 2014.
- [15] T. J. Cui, S. Liu, and L. Zhang, "Information metamaterials and metasurfaces," *J. Mater. Chem. C*, vol. 5, no. 15, pp. 3644–3668, 2017.
- [16] M. K. T. Al-Nuaimi, Y. He, and W. Hong, "Design of 1-bit coding engineered reflectors for EM-wave shaping and RCS modifications," *IEEE Access*, vol. 6, pp. 75422–75428, Nov. 2018.
- [17] H. Sun, C. Gu, X. Chen, Z. Li, L. Liu, B. Xu, and Z. Zhou, "Broadband and broad-angle polarization-independent metasurface for radar cross section reduction," *Sci. Rep.*, vol. 7, Jan. 2017, Art. no. 40782.
- [18] L. Liang, M. Wei, X. Yan, D. Wei, D. Liang, J. Han, X. Ding, G. Zhang, and J. Yao, "Broadband and wide-angle RCS reduction using a 2-bit coding ultrathin metasurface at terahertz frequencies," *Sci. Rep.*, vol. 6, Dec. 2016, Art. no. 39252.
- [19] P. Su, Y. Zhao, S. Jia, W. Shi, and H. Wang, "An ultra-wideband and polarization-independent metasurface for RCS reduction," *Sci. Rep.*, vol. 6, Feb. 2016, Art. no. 20387.
- [20] J. C. I. Galarregui, A. T. Pereda, J. L. M. de Falcón, I. Ederra, R. Gonzalo, and P. de Maagt, "Broadband radar cross-section reduction using AMC technology," *IEEE Trans. Antennas Propag.*, vol. 61, no. 12, pp. 6136–6143, Dec. 2013.
- [21] A. Y. Modi, C. A. Balanis, and C. Birtcher, "Novel technique for enhancing RCS reduction bandwidth of checkerboard surfaces," in *Proc. IEEE Int. Symp. Antennas Propag. USNC/URSI Nat. Radio Sci. Meeting*, Jul. 2017, pp. 1911–1912.
- [22] Y. Zheng, J. Gao, X. Cao, Z. Yuan, and H. Yang, "Wideband RCS reduction of a microstrip antenna using artificial magnetic conductor structures," *IEEE Antennas Wireless Propag. Lett.*, vol. 14, pp. 1582–1585, 2015.
- [23] Y. Li, J. Zhang, S. Qu, J. Wang, H. Chen, Z. Xu, and A. Zhang, "Wideband radar cross section reduction using two-dimensional phase gradient metasurfaces," *Appl. Phys. Lett.*, vol. 104, Jun. 2014, Art. no. 221110.
- [24] F. Yuan, G.-M. Wang, H.-X. Xu, T. Cai, X.-J. Zou, and Z.-H. Pang, "Broadband RCS reduction based on spiral-coded metasurface," *IEEE Antennas Wireless Propag. Lett.*, vol. 16, pp. 3188–3191, 2017.
- [25] S. J. Li, X. Y. Cao, L. M. Xu, L. J. Zhou, H. H. Yang, J. F. Han, Z. Zhang, D. Zhang, X. Liu, C. Zhang, Y. J. Zheng, and Y. Zhao, "Ultra-broadband reflective metamaterial with RCS reduction based on polarization converter, information entropy theory and genetic optimization algorithm," *Sci. Rep.*, vol. 5, Nov. 2016, Art. no. 37409.
- [26] Y. Saifullah, F. Zhang, G. Yang, and F. Xu, "3-bit polarization insensitive reflective metasurface for RCS reduction," in *Proc. 12th Int. Symp. Antennas, Propag. EM Theory (ISAPE)*, Dec. 2018, pp. 1–3.
- [27] S. Sui, H. Ma, J. Wang, Y. Pang, M. Feng, Z. Xu, and S. Qu, "Absorptive coding metasurface for further radar cross section reduction," *J. Phys. D, Appl. Phys.*, vol. 51, no. 6, Jan. 2018, Art. no. 065603.
- [28] S. Sui, H. Ma, Y. Lv, J. Wang, Z. Li, J. Zhang, Z. Xu, and S. Qu, "Fast optimization method of designing a wideband metasurface without using the Pancharatnam–Berry phase," *Opt. Express*, vol. 26, no. 2, pp. 1443–1451, 2018.
- [29] J. Su, H. He, Z. Li, Y. Yang, H. Yin, and J. Wang, "Uneven-layered coding metamaterial tile for ultra-wideband RCS reduction and diffuse scattering," *Sci. Rep.*, vol. 8, May 2018, Art. no. 8182.
- [30] Y. Zheng, X. Cao, J. Gao, H. Yang, Y. Zhou, and S. Wang, "Shared aperture metasurface with ultra-wideband and wide-angle low-scattering performance," *Opt. Mater. Express*, vol. 7, no. 8, pp. 2706–2714, 2017.
- [31] H. Eskandar, A. Sadollah, A. Bahreinejad, and M. Hamdi, "Water cycle algorithm—A novel metaheuristic optimization method for solving constrained engineering optimization problems," *Comput. Struct.*, vols. 110–111, pp. 151–166, Nov. 2012.
- [32] W. Pan, C. Huang, M. Pu, X. Ma, J. Cui, B. Zhao, and X. Luo, "Combining the absorptive and radiative loss in metasurfaces for multi-spectral shaping of the electromagnetic scattering," *Sci. Rep.*, vol. 6, Feb. 2016, Art. no. 21462.
- [33] Y. Zhuang, G. Wang, J. Liang, T. Cai, X.-L. Tang, T. Guo, and Q. Zhang, "Random combinatorial gradient metasurface for broadband, wide-angle and polarization-independent diffusion scattering," *Sci. Rep.*, vol. 7, Nov. 2017, Art. no. 16560.
- [34] Q. Zheng, Y. Li, J. Zhang, H. Ma, J. Wang, Y. Pang, Y. Han, S. Sui, Y. Shen, H. Chen, and S. Qu, "Wideband, wide-angle coding phase gradient metasurfaces based on Pancharatnam–Berry phase," *Sci. Rep.*, vol. 7, Mar. 2017, Art. no. 43543.
- [35] W. Chen, C. A. Balanis, and C. R. Birtcher, "Checkerboard EBG surfaces for wideband radar cross section reduction," *IEEE Trans. Antennas Propag.*, vol. 63, no. 6, pp. 2636–2645, Jun. 2015.
- [36] A. Ghayekhloo, M. Afsahi, and A. A. Orouji, "Checkerboard plasma electromagnetic surface for wideband and wide-angle bistatic radar cross section reduction," *IEEE Trans. Plasma Sci.*, vol. 45, no. 4, pp. 603–609, Apr. 2017.
- [37] A. Edalati and K. Sarabandi, "Wideband, wide angle, polarization independent RCS reduction using nonabsorptive miniaturized-element frequency selective surfaces," *IEEE Trans. Antennas Propag.*, vol. 62, no. 2, pp. 747–754, Sep. 2014.



YASIR SAIFULLAH (S'19) received the B.Sc. and M.Sc. degrees in electrical engineering from the University of Engineering and Technology, Taxila, Pakistan, in 2011 and 2016, respectively. He is currently pursuing the Ph.D. degree with the School of Information Science and Technology, Fudan University, Shanghai, China.

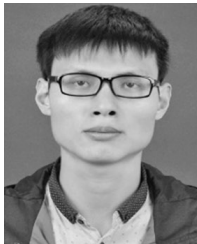
From 2012 to 2013, he was an Operational Engineer with Pakistan Telecommunication Company Limited (PTCL), Pakistan. His research interests include microwave, antenna design, coding, and programmable metasurfaces.



ABU BAKAR WAQAS received the B.Sc. and M.Sc. degrees in electrical engineering from the University of Engineering and Technology, Taxila, Pakistan, in 2011 and 2013, respectively. He is currently pursuing the Ph.D. degree with the School of Information Science and Technology, Fudan University, Shanghai, China. He served his Alma Mater as a Lecturer for four years. His research interests include quantum computation, quantum communications, smart grid, and optimization of electrical engineering problems.

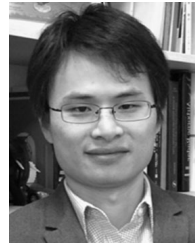


GUO-MIN YANG (S'07–M'10–SM'17) was born in Zhejiang, China. He received the B.S. degree (Hons.) in communication engineering from the Xi'an University of Technology, Xi'an, China, in 2002, the M.S. degree in electronic engineering from Shanghai Jiao Tong University, Shanghai, China, in 2006, and the Ph.D. degree in electrical and computer engineering from Northeastern University, Boston, MA, USA, in 2010. In 2010, he joined the Faculty of the School of Information and Technology, Fudan University, where he is currently an Associate Professor. He has authored 46 journal publications and 40 conference articles. His research interests include antenna miniaturization, magneto-dielectric materials, metamaterials, frequency selective surfaces, microwave wireless power transfer, RF energy harvesting, and inverse scattering problems in electromagnetics.



FUHENG ZHANG received the B.E. degree in electronic engineering from the Changshu Institute of Technology, Suzhou, China, in 2012. He is currently pursuing the Ph.D. degree with the Key Laboratory for Information Science of Electromagnetic Waves, Fudan University, Shanghai, China.

His research interests include wideband microstrip antenna design and synthesis, metasurface design and synthesis, and signal integrity.



FENG XU (S'06–M'08–SM'14) received the B.E. degree (Hons.) in information engineering from Southeast University, Nanjing, China, in 2003, and the Ph.D. degree (Hons.) in electronic engineering from Fudan University, Shanghai, China, in 2008.

From 2008 to 2010, he was a Postdoctoral Fellow with the NOAA Center for Satellite Application and Research, Camp Springs, MD, USA. From 2010 to 2013, he was with Intelligent Automation Inc., Rockville, MD, USA. He was a Research Scientist with the NASA Goddard Space Flight Center, Greenbelt, MD, USA. He is currently a Professor with the School of Information Science and Technology and the Vice Director with the MoE Key Laboratory for Information Science of Electromagnetic Waves, Fudan University. He has authored more than 30 articles in peer-reviewed journals, coauthored two books, and holds two patents, among many conference articles. His research interests include electromagnetic scattering modeling, SAR information retrieval, and radar system development.

Dr. Xu was a recipient of the Second-Class National Nature Science Award of China, in 2011, the Early Career Award of the IEEE Geoscience and Remote Sensing Society, in 2014, and the SUMMA Graduate Fellowship in the advanced electromagnetics area, in 2007. He is currently the Founding Chair of the IEEE GRSS Shanghai Chapter, which was awarded as the GRSS Best Chapter, in 2017. He also serves as an Associate Editor for the IEEE GEOSCIENCE AND REMOTE SENSING LETTERS.

...